Journal of the Nigerian Association of Mathematical Physics
Volume 48 (*Sept. & Nov., 2018 Issue*), pp209 –218

A GENERAL POTENTIAL FOR MOLECULAR DYNAMICS OF ION-SPUTTERED SURFACES

[*]Akande Raphael O. and[†]Oyewande Emmanuel O.

[*]Theoretical Physics Group, Mountain Top University, Ogun State, Nigeria.
[†]Theoretical Physics Group, Department of Physics, University of Ibadan, Ibadan, Nigeria.

Abstract

Erosion of surface atoms of solid materials by ion bombardment (surface-sputtering) causes nano-ripples and quantum dots to self-organize on the surfaces. The self-organization had been shown, in some sputtering experiments, to be influenced by unexpected contaminants (ions) from vacuum walls. Existing inter-atomic-interaction potentials of Molecular Dynamics (MD) simulations for studying this are unsuitable because they assume two-particle collisions at a time instead of many (including contaminants)-particle collisions (Wider-area Perturbations, (WP)). We designed this study to develop a suitable potential that incorporates WP of the MD. We developed the general potential to account for the possibility of WP due to contaminants (both foreign and local to the material) consequently shifting the equilibrium points of the MD of the material. For instance, dynamics of Au and Fe were studied with O bombardments/contamination (oxygenated environments), and those of CSiGe were studied with W, Ti, and O. It was found that the phase-shift, of the equilibrium points of the MD simulations, for Au stabilized for just five atoms of oxygen while that of Fe did not, when interacting in separate oxygenated environments. A different phase shift was recorded for CSiGe which reflected the usage of different contaminants, under subsequent bombardments with W, Ti and O, in transformations to CSiGeW, CSiGeWTi, and CSiGeWTiO. These results and those for the sampled superconducting materials, such as SrNdCuO and LiFeAs, showed a sensitivity of the general potential, and insensitivity of the existing potentials, to the type and environment of the atoms of these materials. Furthermore, results obtained clearly show that the MD perturbations in a material, via its surface, are peculiar to the surface and that the MD is actually dynamic.

Keywords: Potential; surfaces; repulsion, scattering and sputtering; molecular dynamics perturbation; material processing

1. Introduction

The industrial and research understanding of atomic interactions often ignore some perturbations of the molecular dynamics. Some readily available applications, which indicate these perturbations, can be found in the solar panel surface sputtering which is also an important factor in its effectiveness, thus the need for anti-reflective coats on its surface [1]. Even the best of water and chemical proof materials [2] and materials that will one day allow us to breathe under water are now being developed [3] but little or no attention is given to the dynamics of these materials' molecular dynamics. Many a times there are different degrees of energy absorption on different surfaces. Biological surfaces' energy spread differs from that of the inorganics, this is why it is important to design chemically inert surfaces [4] and develop artificial Antimicrobial Activity of Water Resistant Surface Coating [5]. In some other applications, nano-scale energy transport might not be required. However, in others like the biological surfaces, there is a need to study nano-scale energy transport so as to effectively monitor the delivery of energy/drugs to the active sections of organs.

1.1 Problem statement and motivation for research

In this work, we want to incorporate the processes on sputtered surfaces [6,7,8] to molecular interactions [9] so as to illustrate our proposal that the molecular dynamics of materials is in itself a dynamic process. We have chosen sputtered surfaces because of their resemblance to natural form of interactions which is often by collision.

Corresponding Author**:** Akande R.O., Email: roakande@mtu.edu.ng, Tel: +2348131597032, +2347066577984 (OEO)

Materials are not operating in isolation from their environments. While the material is undergoing molecular dynamics (within its bulk), its surface is always being bombarded with foreign particles. In essence, the current molecular dynamics is perturbed [10] by the energies thrown downwards by the approaching foreign particles. Therefore, all materials are in constant tune with their environments, which implies that we must develop a potential for the molecular interactions to incorporate this surface sputtering section of the interactions. We are convinced that the molecular dynamics perturbations in a material, as a result of bombardments on its surface by foreign particles, are peculiar to the surface. The essence of developing a general potential is to be able to apply the single potential to any (or most) materials located in any environment. In what follows, we discuss some potentials in literature which are not general enough for achieving our goal.

1.2 Interatomic Potentials for Metallic Systems

We shall itemize the well-known potentials as follows, source: [13]:

$$H_I^{EAM} = \sum_i F_i[\rho_{h,i}] + \frac{1}{2}\sum_i \sum_{j\neq i} \emptyset_{ij}(r_{ij}) \dots\dots\dots\dots\dots\dots\dots\dots\dots\dots\dots\dots\dots\dots\dots\dots (1a)$$

Equation (1a) is the Many-Body Embedded-Atom Model (EAM) Potentials, where $\rho_{h,i}$ is the electron density of the host at the site of atom i, $F_i[\rho_{h,i}]$ is the embedding functional, that is, the energy to embed an extra atom i, into the background electron density,ρ and$\emptyset_{ij}$ is a pairwise central potential between atoms i and j, separated by a distance r_{ij}. $\emptyset_{ij}$ represents the repulsive core-core electrostatic interaction. The electron density of the host lattice is a linear superposition of the individual contributions and is given as:

$$\rho_{h,i} = \sum_{j\neq i} \rho_j^*(r_{ij}) \dots\dots\dots\dots\dots\dots\dots\dots\dots\dots\dots\dots\dots\dots\dots\dots\dots\dots\dots\dots\dots\dots (1b)$$

whereρ_j^* is also a pairwise term and is the electron density of atom j as a function of interatomic separation.The EAM are developed based on existing Density Functional Theory (DFT). According to DFT, the energy of a collection of atoms can be expressed exactly by a functional of its electronic density.

$$H_I^{FS} = \frac{1}{2}\sum_{i\to N}\sum_{j\neq i} V(r_{ij}) - c\sum_i (\rho_i)^{1/2} \dots\dots\dots\dots\dots\dots\dots\dots\dots\dots\dots\dots\dots\dots\dots\dots (2)$$

Equation (2) is the Many-Body Finnis-Sinclair (FS) potentials developed with the intention to model the energetics of the transition metals. They offer a better description of the surface relaxation in metals. They also avoid problems, such as the appearance of the Cauchy relation between the elastic constants $C_{12} = C_{44}$which is not satisfied by cubic crystals, associated with using pair potentials to model metals.

In equation (2), $\rho_i = \sum_{j\neq i} \emptyset_{ij}(r_{ij}) \dots\dots (2b)$, $V(r_{ij})$ is a pairwise repulsive interaction between atoms i and j, separated by a distance r_{ij}. Also, $\emptyset_{ij}(r_{ij})$ are the two-body cohesive pair potentials, and c is a positive constant. The second term in (2) is the cohesive many-body contribution to the energy.

$$H_I^{SC} = \varepsilon\left[\frac{1}{2}\sum_i\sum_{j\neq i} V(r_{ij}) - c\sum_i (\rho_i)^{1/2}\right] \dots\dots\dots\dots\dots\dots\dots\dots\dots\dots\dots\dots\dots (3a)$$

Equation (3a) is the Many-Body Sutton-Chen (SC) Long-Range Potentials. They only describe the energies of 10 fcc elemental metals. They are similar to the FS type potentials and also similar to EAM potentials in form. SC potentials are very good for computer simulations of nanostructures involving large number of atoms, where ε is a parameter with the dimensions of energy,

$$V(r_{ij}) = \left(\frac{a}{r_{ij}}\right)^n \dots\dots\dots\dots\dots\dots\dots\dots\dots\dots\dots\dots\dots\dots\dots\dots\dots\dots\dots\dots\dots\dots (3b),$$

$$\rho_i = \sum_{j\neq i}\left(\frac{a}{r_{ij}}\right)^m \dots\dots\dots\dots\dots\dots\dots\dots\dots\dots\dots\dots\dots\dots\dots\dots\dots\dots\dots\dots\dots\dots (3c)$$

Where a is a parameter with the dimensions of length and usually means the equillibrium lattice constant.$m$and$n$ are positive integers with $n > m$. The power law form was adopted so as to enable the model to be unique in combining the short-range interactions (due to the$N$-body second term of (3a)) and good for describing the surface relaxation phenomena using a van der Waals tail which gives a better description of the long-range interactions.

$$U_{tot} = \sum_i\sum_{j>i} U_{ij}^{(2)} - \sum_i\sum_{j>i}\sum_i U_{ijk}^{(3)} \dots\dots\dots\dots\dots\dots\dots\dots\dots\dots\dots\dots\dots\dots\dots\dots\dots (4a)$$

Equation (4a) is the Many-Body Murrel-Mottram (MM) Potentials. They are examples of cluster-type potentials and consist of sums of effective two- and three-body interactions. The pair interaction term, that is the first term, is modeled by a Rydberg function, which has been used for simple diatomic potentials. The first term takes the form below:

$$\frac{U_{ij}^{(2)}}{D} = -(1 + a_2\rho_{ij})exp(-a_2\rho_{ij}) \dots\dots\dots\dots\dots\dots\dots\dots\dots\dots\dots\dots\dots\dots\dots\dots\dots (4b)$$

where $\rho_{ij} = \frac{r_{ij}-r_e}{r_e}$. D is the depth of the potential minimum, corresponding to the diatomic dissociation energy are $\rho_{ij} = 0$, for $r_{ij} = r_e$, where r_e is the diatomic equilibrium distance.

$$\frac{U_{ij}^{(3)}}{D} = P(Q_1, Q_2, Q_3)F(a_3, Q_1) \ldots \ldots (4c)$$

Where

$$P(Q_1, Q_2, Q_3) = c_0 + c_1Q_1 + c_2Q_1^2 + c_3(Q_2^2 + Q_3^2) + c_4Q_1^3 + c_5Q_1(Q_2^3 + Q_3^2) + c_6(Q_3^3 - 3Q_3Q_2^2) \ldots \ldots (4d)$$

From equation (4d), it implies that there are seven unknowns in this model. $F(a_3, Q_1)$ is the damping function and can take the following three forms:

$$F(a_3, Q_1) = exp(a_3Q_1) \ldots \ldots (4e),$$

$$F(a_3, Q_1) = \frac{1}{2}\left[1 - tanh\left(\frac{a_3Q_1}{2}\right)\right] \ldots \ldots (4f)$$

$$F(a_3, Q_1) = sech(a_3Q_1) \ldots \ldots (4g),$$

The coordinates Q_i are given as:

$$\begin{bmatrix} Q_1 \\ Q_2 \\ Q_3 \end{bmatrix} = \begin{vmatrix} \sqrt{1/3} & \sqrt{1/3} & \sqrt{1/3} \\ 0 & \sqrt{1/2} & -\sqrt{1/2} \\ \sqrt{2/3} & -\sqrt{1/6} & -\sqrt{1/6} \end{vmatrix} \begin{bmatrix} \rho_{ij} \\ \rho_{jk} \\ \rho_{ki} \end{bmatrix} \ldots \ldots (4h)$$

$$U_{RTS} = \frac{1}{2}\sum_i \sum_{j \neq i} \hat{p}_i\hat{p}_j V_{AA}(r_{ij}) + (1-\hat{p}_i)(1-\hat{p}_j)V_{BB}(r_{ij}) + [\hat{p}_i(1-\hat{p}_j) + \hat{p}_j(1-\hat{p}_i)]V_{AB}(r_{ij})$$
$$- d^{AA}\sum_i \hat{p}_i \left[\sum_{i\neq j} \hat{p}_j \Phi_{AA}(r_{ij}) + (1-\hat{p}_j)\Phi_{AB}(r_{ij})\right]^{1/2}$$
$$- d^{BB}\sum_i (1-\hat{p}_i) \left[\sum_{i\neq j} (1-\hat{p}_j)\Phi_{BB}(r_{ij}) + \hat{p}_j \Phi_{AB}(r_{ij})\right]^{1/2} \ldots \ldots (5a)$$

Equation (5a) is the Many-Body Rafii-Tabar-Sutton (RTS) Long-Range Alloy Potentials. They are, in particular, good for $A - A$, $A - B$and $B - B$fcc alloy metals. The RTS potentials are a form of generalization of the SC potentials and they model the energetics of the metallic fcc (face centered crystal) random binary alloys. They have the advantage of having little unknown parameters.

In equation (5a),

$$V_{\alpha\beta}(r) = \varepsilon^{\alpha\beta}\left[\frac{a^{\alpha\beta}}{r}\right]^{n_{\alpha\beta}} \ldots \ldots (5b),$$

$$\Phi_{\alpha\beta}(r) = \left[\frac{a^{\alpha\beta}}{r}\right]^{m_{\alpha\beta}} \ldots \ldots (5c)$$

where α, β may be A and B. The parameters ε^{AA}, c^{AA}, a^{AA}, m^{AA} and n^{AA} are for the pure element A, while the parameters ε^{BB}, c^{BB}, a^{BB}, m^{BB} and n^{BB} are for the pure element B.

also $d^{AA} = c^{AA}\varepsilon^{AA}$, $d^{BB} = c^{BB}\varepsilon^{BB}$ …… (5d)

The mixed or pure alloy states or forms are contained in the following combining rules:

$$V_{AB} = (V^{AA}V^{BB})^{1/2}, \; \Phi_{AB} = (\Phi^{AA}\Phi^{BB})^{1/2}, \; m^{AB} = \frac{1}{2}(m^{AA} + m^{BB})$$

$$n^{AB} = \frac{1}{2}(n^{AA} + n^{BB}), \; a^{AB} = (a^{AA}a^{BB})^{1/2}, \; \varepsilon^{AB} = (\varepsilon^{AA}\varepsilon^{BB})^{1/2} \ldots \ldots (5e)$$

These parameters are very crucial to the MD simulations of elastic constants and heat of formation of a set of fcc metallic alloys as well as for modeling the ultra-thinPd films on a Cu(100) surface.

The operator $\hat{p}_i$ is the site occupancy operator and is defined as:

$\hat{p}_i = 1$, *if the site i is occupied by an atom A*

$\hat{p}_i = 0$, *if the site i is occupied by an atom B*

2. Methods

2.1 Making the potential general

To make the potential general for studying the perturbation of the molecular dynamics, due to energies delivered into a material by sputtering ion(s), we want to relate the following, listed, processes to one another. The reason being that the following are related in sequential manner. It is our belief that these processes are needed and are common to most materials.

1. the location of the landing ions will be called a sputtered location,
2. the sputtered location is the origin of a nano-scale energy transport spreading in all directions and into the bulk,
3. all atoms captured by the energy spread will be regarded as the captured atoms,
4. it is important to note that there could be different atomic elements within the captured space,
5. the transportation of this energy causes ionizations of the captured atoms. Different atomic elements will receive and respond to this energy differently,
6. we plan to apply the, rapidly changing, PAPCs (Photon Absorption Potential Coefficient as described in [15]) of each atom in that captured space to study the variations in the way each atom receives energy,
7. we assume that even the same atoms, but located at different positions, in the sputtered location would become different due to PAPCs,
8. then we provide a way to evaluate the energy of the captured atoms in the, growing, sputtered location.

Now, we concentrate on the development of two very crucial parameters:

i. the rate at which the number of ionized atoms increases and decreases due to the energy delivered by the sputtering particles landing on the surface and
ii. the PAPC, which is essential in making the potential a general one.

2.2 Number of ionized atoms

We could calculate the number of atoms that could be ionized by such energies as:

$$N_{\text{ionized atoms}} = \frac{E_{ion}}{\sum_i^N I_i} \quad (6)$$

whereE_{ion} is the energy of the incoming ion and I_i are the ionization energies of the atoms in the lattice. For ionic lattices like that of NaCl, we could have two unique forms ofI_i, that is: $I_\alpha$and I_β. Therefore, equation (6) becomes

$$N_{\text{ionized atoms}} = N_{\alpha\text{ atoms}} + N_{\beta\text{ atoms}} = \frac{E_{ion}}{\sum_\alpha^{N_\alpha} I_\alpha + \sum_\beta^{N_\beta} I_\beta} \quad (7)$$

Since we are looking at both laboratory and general cases of materials, we shall consider cases where the atomic lattice is very irregular (not necessarily amorphous) as well. In such cases (examples include a material made up of different homogenous layers of atoms), we have atomic arrangements where, say the α atoms are grouped together, more at a point, than at others. Same is applicable to irregular mixtures for $\beta, \gamma,$ ....atoms. For such complex molecules we have:

$$N_{\text{ionized atoms}} = N_{\alpha\text{ atoms}} + N_{\beta\text{ atoms}} + \cdots = \frac{E_{ion}}{\sum_\alpha^{N_\alpha} I_\alpha + \sum_\beta^{N_\beta} I_\beta + \cdots} \quad (8)$$

Please note that we cannot write (7 and 8) as :

$$N_{\text{ionized atoms}} = \frac{E_{ion}}{N_\alpha I_\alpha + N_\beta I_\beta + \cdots} \quad (9)$$

because

1. even though the $\alpha, \beta,$... atoms are fundamentally the same, they are electronically different at any point in time.
2. the direction or path along which the atoms receive energy must also be considered in determining how much of energy is left for subsequent ionizations.
3. the atoms might not be located close to one another at equal distances,
4. it is also important that we discuss the fact that the population of ionized atoms is always changing in the lattice. This is because initially as the sputtering process starts, there are a larger number of first ionization atoms but as the sputtering process increases, we have that number reducing while the number of nth ionization atoms also increases.
5. the point, just above, is what we have identified as a major reason why contributions to sputtering yield by temperature variations is crucial to a successful model for surface interactions. Research works on the contributions of temperature rise to sputtering yield is scarce and the very few model for such case is stated as follows [14]:

$$\lambda \sim \frac{1}{T^{1/2}} exp\left(-\frac{\Delta E}{2k_B T}\right) \quad (10)$$

whereλ is the ripple wavelength, T is the temperature, ΔE is the activation energy of the system and k_B is the Boltzmann's constant.

Let us consider, for now, two groups of ionizations: first and second ionizations. The first ionization is handled as :

$$N_{\text{first ionized atoms}} = N_1 = 1 - tanh(\xi) \quad (11)$$

and the second as :

$$N_{\text{second ionized atoms}} = N_2 = tanh(\xi) \quad (12)$$

As ξ increases, the N_1 reduces and N_2 increases. Equations 11 and 12, above are similar to:

$N_{\text{second ionized atoms}} = N_2 = N - N_1 \ldots\ldots\ldots\ldots\ldots\ldots\ldots\ldots\ldots\ldots (13)$
where N is the total number of atoms in the lattice, assuming that we can only have two (first and second) ionizations.
In general, for a complex system, we have:

$$N_{\text{first ionized atoms}} = N_{ij} = N_1\left(\delta_{ij} + \frac{(-1)^{ij}}{2} tanh(\xi)\right) \ldots\ldots\ldots\ldots\ldots (14)$$

$$N_{\text{second ionized atoms}} = N_{jk} = N_2\left(\delta_{jk} + \frac{(-1)^{jk}}{2} tanh(\xi)\right) \ldots\ldots\ldots\ldots\ldots (15)$$

$$N_{\text{third ionized atoms}} = N_{kl} = N_3\left(\delta_{kl} + \frac{(-1)^{kl}}{2} tanh(\xi)\right) \ldots\ldots\ldots\ldots\ldots (16)$$

$$N_{\text{nth ionized atoms}} = N_{nm} = N_{nth}\left(\delta_{nm} + \frac{(-1)^{nm}}{2} tanh(\xi)\right) \ldots\ldots\ldots\ldots (17)$$

So we have:
$N_{\text{ij}} = N_1 + N_2 \Rightarrow N_2 = N_{\text{ij}} - N_1$
$N_{\text{jk}} = N_2 + N_3 \Rightarrow N_3 = N_{\text{jk}} - N_2$
$N_{\text{kl}} = N_3 + N_4 \Rightarrow N_4 = N_{\text{kl}} - N_3$
…
$\therefore\ N_3 = N_{jk} - \left(N_{ij} - N_1\right) = N_{jk} - N_{ij} - N_1 \ldots\ldots\ldots\ldots\ldots\ldots\ldots\ldots (18)$
$N_4 = N_{kl} - N_{jk} + N_{ij} - N_1 \ldots\ldots\ldots\ldots\ldots\ldots\ldots\ldots\ldots\ldots (19)$
$N_5 = N_{lm} - N_{kj} + N_{jk} - N_{ij} + N_1 \ldots\ldots\ldots\ldots\ldots\ldots\ldots\ldots\ldots (20)$
…

Please note that $N_4, N_5, N_6, \ldots$ population will be ≈ 0at the initial stages of the sputtering process. As time factor ξ grows, N_4, N_5, N_6 will start emerging while N_3, N_2, N_1start disappearing.
Now, we can re-write equation (8) as:

$$N_{\text{ionized atoms}} = \frac{E_{ion}}{N_{pq} - \cdots N_{lm-N_{kl}} + N_{jk} - N_1} \ldots\ldots\ldots\ldots\ldots\ldots\ldots\ldots (21)$$

i. Please note that ξ is the condition of time frame during the whole process of sputtering,
ii. Also, we shall define δ_{ij} , δ_{jk} , ...as the conditions for the transfer of ionization from one stage to another,
iii. the $\frac{1}{2}$in equations (14) to (17) is for the purpose of linking one stage of ionization to the other,
iv. the$N_1, N_2, \ldots$ in equations (14) to (17) are the initial numbers of each stage of ionization.

2.3 Introducing the PAPC
PAPC is our way of finding out the way similar (such as two Na atoms but at different ionizations) or different (such as Na and Cl atoms at the same or different ionizations) atoms would react to the energy delivered by the sputtering ion(s). Therefore, we arrive at the following:

$$A_c = \frac{1}{2z}\left\{ln\left(\frac{1+z^-}{1-z^-}\right) + ln\left(\frac{1+z^+}{1-z^+}\right)\right\} \ldots\ldots\ldots\ldots\ldots\ldots\ldots\ldots (22)$$

Equation (22) can also be written as:

$$A_c = \frac{1}{z}\{tanh(z^-) + tanh(z^+)\} \ldots\ldots\ldots\ldots\ldots\ldots\ldots\ldots (23)$$

where$z^-$is given as:$z^- = \frac{z_v^-}{|z-z_v^-|} \ldots\ldots\ldots\ldots\ldots\ldots\ldots\ldots (24)$
andz^+ is given as:$z^+ = \frac{z_v^+}{|z-z_v^+|} \ldots\ldots\ldots\ldots\ldots\ldots\ldots\ldots (25)$
wherez_v^+ and z_v^- are the extra subtracted and added electrons of the neutral atom in question. Take for instance, the A_c of an atom like Na is will be given as:

i. for first ionization, we have:$z_v^+ = \frac{12}{|11-12|} = 12,\ and\ z_v^- = \frac{10}{|11-10|} = 10$
ii. for second ionization, we have:$z_v^+ = \frac{13}{|11-13|} = 6.5,\ and\ z_v^- = \frac{9}{|11-9|} = 4.5$
iii. for third ionization, we have:$z_v^+ = \frac{14}{|11-14|} = 4.6667,\ and\ z_v^- = \frac{8}{|11-8|} = 0.05562$

2.4 Derivations for the general potential
To further study this perturbation, we apply the principle that the energy thrown off (radiation beamed at the surface) by the, gradually, approaching foreign particle captures and causes an ionization of a group of atoms on the surface. This, group, ionization leads to a buildup of a forceful repulsive energy amongst the captured atoms. This repulsion eventually translates to surface sputtering and penetration of the incoming particle. Therefore, this incoming particle's energy does work on the surface of the material it approaches. To this end, we introduce the proposed work done on the surface by the incoming beams of ions. Before we state the proposed work done, we state the repulsion potential suitable for our work done, comparable to those well-known potentials such as Lennard-Jones' and Morse's [11,12], as follows:

$$\Upsilon = \gamma\left(e^{\left(\frac{1}{\pi\sigma}\right)} - \frac{\hat{k}\hat{\mu}}{\gamma^2}\right)\Gamma(\zeta) \ldots\ldots\ldots(26)$$

where

$\gamma$is the energy of the incoming ion,

$\sigma \to \sigma_{i+1} = \sigma_i + \Delta\sigma$, [$where\ \Delta\sigma = exp\left(\frac{-\gamma}{\theta\sigma}\right)$]is the area covered by the photon cone of the ion. If the sputtering angleθ which can take values from 0 and 90 degrees, is 0 (meaning that the approach on the surface is perpendicular to the surface), then we have $\Delta\sigma = 0$.

$$\hat{k} = \frac{k\ region}{\sum atomic\ diameters\ of\ atoms\ in\ k\ region} = \frac{k\ region}{\sum D_{pq} - \cdots \sum D_{lm} - \sum D_{kl} + \sum D_{jk} - \sum D_{ij} + \sum D_1}$$

$\hat{k}$is the lattice site occupation density of the topograph of the surface in which the ion is to land. Please note that the default $k$region for a flat surface is a circular shape. Where $\sum D_{pq}$ is the sum of all the diameters of atoms in the N_{pq} population.Same explanation is applicableto other similar symbols.

$$\hat{\mu} = A_c \times atomic\ number \ldots\ldots\ldots(27)$$

Equation (27) is the property of the molecules on which the ion is to land. The properties are the PAPC, A_c, and the atomic numbers of the atoms of that molecule, where PAPC is given as earlier stated.

$$A_r = A_c \frac{e}{R}$$

$A_r$is the rate of change of A_c with distance R, $e$is the electronic charge and R isthe increasing distance of the transporting energy from the landing site of the foreign particle.

$$\zeta = \beta\hat{\mu}\sigma \ldots\ldots\ldots(28)$$

Equation (28) is the quantity that determines the activation of the sputtering as the ion is approaching the surface. $\beta$is a constant that stabilizes the rate of increment or reduction of σ,

$$\Gamma(\xi) = 1 - tanh(\xi) \ldots\ldots\ldots(29)$$

Equation (29) helps to activate the sputtering process. This is because when the ion is still far off, above the surface, there will not be sputtering but as it approaches the surface, the sputtering process starts to build up, gradually. Please see Figure 1 for illustrations.

Therefore, we may wish to write:

$$\Upsilon = \gamma\left(e^{\left(\frac{1}{\pi\sigma}\right)} - \frac{\hat{\mu}\int d^3\sigma}{\gamma^2\sum_i D_i}\right)\Gamma(\zeta) \ldots\ldots\ldots(30)$$

whereD_i are the diameters of the atoms in the k region.
Finally, we now have the proposed work done on the surface, by one ion's photon shower, to be given as:

$$\Omega = \sigma\frac{d\Upsilon}{d\sigma} \ldots\ldots\ldots(31)$$

$$\Omega = \gamma exp\left(\frac{1}{\pi\sigma^2}\right) - \frac{\sigma\hat{\mu}\partial_\sigma\int d^3\sigma}{\gamma^2\sum_i D_i} - \left(\gamma exp\left(\frac{1}{\pi\sigma^2}\right) - \frac{\sigma\hat{\mu}\partial_\sigma\int d^3\sigma}{\gamma^2\sum_i D_i}\right)tanh(\beta\hat{\mu}\sigma) - \left(\gamma exp\left(\frac{1}{\pi\sigma^2}\right) - \frac{\hat{\mu}\partial_\sigma\int d^3\sigma}{\gamma^2\sum_i D_i}\right)\beta\hat{\mu}\sigma\, sech^2(\beta\hat{\mu}\sigma) \ldots\ldots\ldots(32)$$

We present the plots of our derived repulsion potential, for some selected (flat) surfaces at $\gamma = 10eV$, $k$region is $\frac{2}{3}\pi\sigma^3$ and $\beta = 0.5$, as a way to compare with the parameters of the repulsion potentials such as Lennard-Jones' and Morse's.

2.5 Steps taken in applying equation (26)
In order to be non-biased and influenced by well-known results of well-known and well-researched materials, we selected the materials (we worked on) at random without any background information fore-known. The materials are: CSiGe, CSiW, CSiO, WTiO and TiO and figures 4 to 8 are the plots of the applications of our derived potentials for each of them. Then we simulated the bombardment of a seed material, CSiGe, with W, Ti and O, in turn. The intention was to observe, if any, the

variation or perturbation of the MDs of each of the newly formed material after each stage of bombardment. The seed material transforms, after penetrations/perturbations of MD to: CSiGeW, CSiGeWTi, and CSiGeWTiO.

3. Results and conclusion

3.1 Explanations of the results of simulations

The results of the simulation of equation (26) or (30) are presented in the diagrams that follow. Figures 1 and 2 illustrate how energy interactions with the surface are in phases. Real sputtering is activated, gradually, as it gets closer to the surface. The circular shapes are the, default, gradual energy spreads. Figures 3 to 8 are plots of the repulsive potentials against the repulsion distances σ. They are comparisons between the literature (Lennard-Jones' and Morse's potentials) and our proposed potential. In all the figures, $\gamma = 10eV$ and $\frac{2}{3}\pi\sigma^3$. We do not consider the mixing ratios of the alloys and so our figures 3 to 9 do not have any specific molecular formula. Tables 1, 2 and 3 show more comparison between this paper and the literature on the results of simulations carried out on other sampled materials. Figures 9 and 10 are the plots of phase shift in the perturbed molecular dynamics of the materials considered. They show that all materials have frequently changing (perturbed) molecular dynamics as it experiences surface bombardments. In figure 10, the two plots suggest, using our study of the perturbation of the molecular dynamics in materials as, a (probable) reason why Gold does not rust as easily as Iron.

3.2 Conclusions proper

A phase shift was recorded for CSiGe and each of CSiGeW, CSiGeWTi, and CSiGeWTiO which is no doubt due to the perturbation of the MD at each stage of the transformation of the seed material, see figure 9. The same trial/computation was made for Gold and Iron materials under Oxygen bombardment. The conclusion is that there is no further (major) perturbation in the MDs of Gold material to subsequent bombardments beyond 5 Oxygen atoms. On the contrary, there is still a continuous perturbation in the MDs of Iron material beyond the 5th Oxygen bombardments, see figure 10.

It is a well-known fact that materials age, become weak, change color amongst other things but no model, until now, addresses that issue. The derived potential is a single model for simulating the, although known to be present but not modeled, perturbation of MD. The model is also applicable to as many materials as possible as our results suggest. Going by the results obtained, the MD perturbations in a material, via its surface, is peculiar to the surface and itself is also dynamic. We do not consider whether the trend of the perturbation is increasing or decreasing because the trend is due to so many factors listed as parameters of equation (26). We, however, identified up to five different types of repulsions, see figure 11. These different degrees of repulsions are peculiar to a material's surface atoms and hence, a determinant of the type of molecular dynamics such material might subsequently experience. This knowledge will help us study how materials respond to stresses, aging, change in color and most especially to design sensors to determine a change of environment or presence of some toxic substances and many more.

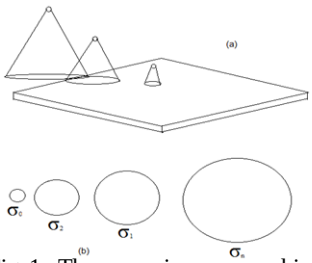

Fig 1: The same ion approaching the surface at slant angles.

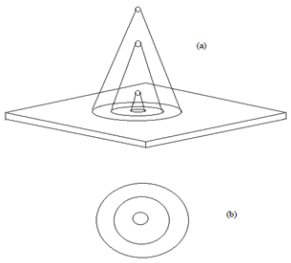

Fig 2: The same ion at normal to the surface.

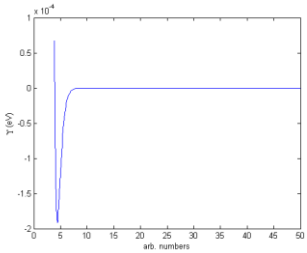

Fig 3: Solution of equation (30) for CSiGeWTiO. The equilibrium position is at$\sigma = 4$. This is a case of quintenary alloy surface.

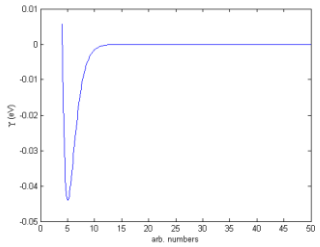

Fig 4: Solution of equation (30) for CSiW. The equilibrium positions are at$\sigma = 4, 4, 4.1, 3.8$respectively. This is a case of tertiary alloy surface or material.

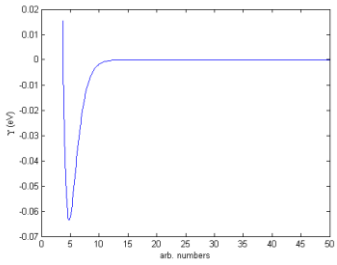

Fig 5: Solution of equation (30) for CSiO. The equilibrium positions are at $\sigma = 4, 4, 4.1, 3.8$ respectively.

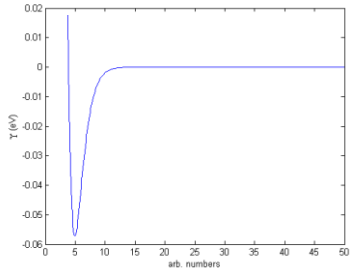

Fig 6: Solution of equation (30) for WTiO. The equilibrium positions are at $\sigma = 4, 4, 4.1, 3.8$respectively. These are other cases of tertiary alloy surface or material.

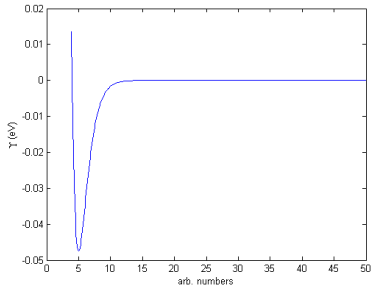

Fig 7: Solution of equation (30) for CSiGe. The equilibrium positions are at $\sigma = 4, 4, 4.1, 3.8$respectively. This is another case of tertiary alloy surface or material.

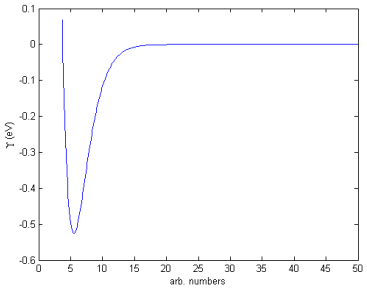

Fig 8: Solution of equation (30) for TiO. The equilibrium position is at $\sigma = 3.8$. This is a case of binary alloy surface.

Table 1: Minimum values for each of the figures. Comparing the results of Morse's, Lennard-Jones' and our potential for Argon.

Potential	**Value**	σ/nm
Morse's	-0.942869	3
Lennard-Jones'	-0.0110927	3
Our potential	-17.2711	98(2)

Table 2: Comparing ***left:*** Morse's with ***right:*** our potential, $\beta = 0.00003$.

Morse's Potential			**Our Potential**	
Material	$Potential/eV$	σ/nm	$Potential/eV$	σ/nm
Tungsten	-0.989553	2	-16746.0	98(2)
Zinc	-0.154966	2	-3916.38	95(5)
Copper	-0.327924	2	-4812.23	95(5)

Table 3:Comparing ***left***Lennard-Jones' with***right*** our potential

Lennard-Jones' Potential			**Our Potential**		
Material	$Potential/eV$	σ/nm	***Material***	$Potential/eV$	σ/nm
SF_6	-207.007	5	$SF_6, \beta = 0.0003$	-38.2094	98(2)
CS_2	-402.091	4	$CS_2, \beta = 0.0003$	-38.3425	98(2)
NH_3	-244.099	3	$NH_3, \beta = 0.003$	-23.2576	96(4)
H_2O	-502.195	2	$H_2O, \beta = 0.003$	-1.88068	98(2)
CH_3CN	-486.32	4	$CH_3CN, \beta = 0.003$	-3.30931	97(3)
$Si(CH_3)_4$	-313.775	6	$Si(CH_3)_4, \beta = 0.0003$	-218.492	96(4)

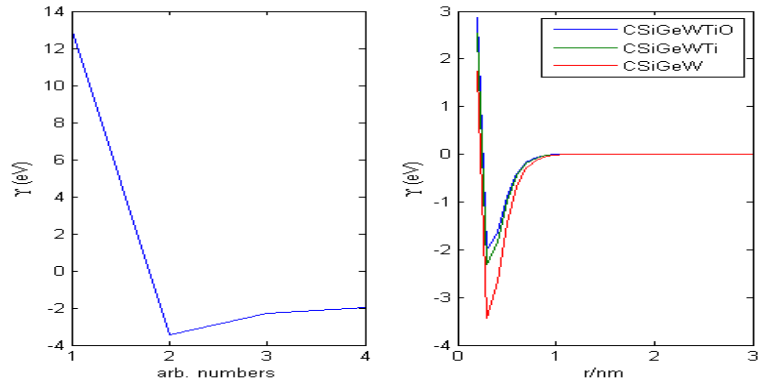

Fig 9: ***right***: Potential plot for CSiGeWTiO, CSiGeWTi and CSiGeW. ***left***: Phase shift in the molecular dynamics of the changing potential in the binding process from CSiGe to CSiGeW to CSiGeWTi and to CSiGeWTiO at the same distance 0.3nm starting with CSiGe.

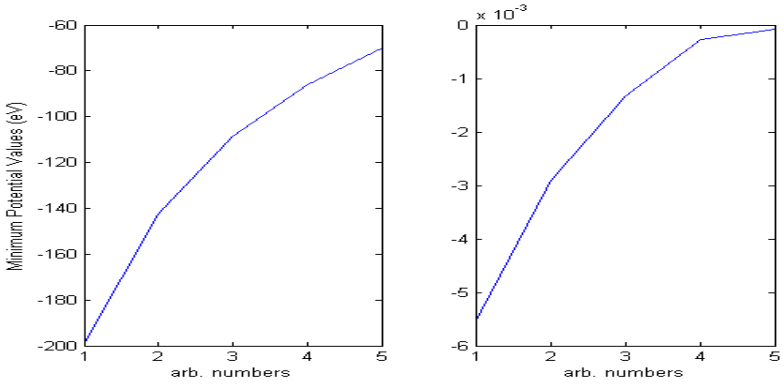

Fig 10: ***right***: Plot of the minimum (equilibrium) potential for transformation from $Au \rightarrow Au + O \rightarrow Au + 2O \rightarrow \cdots \rightarrow Au + 5O$. ***left***: Plot of the minimum (equilibrium) potential for transformation from $Fe \rightarrow Fe + O \rightarrow Fe + 2O \rightarrow \cdots \rightarrow Fe + 5O$.

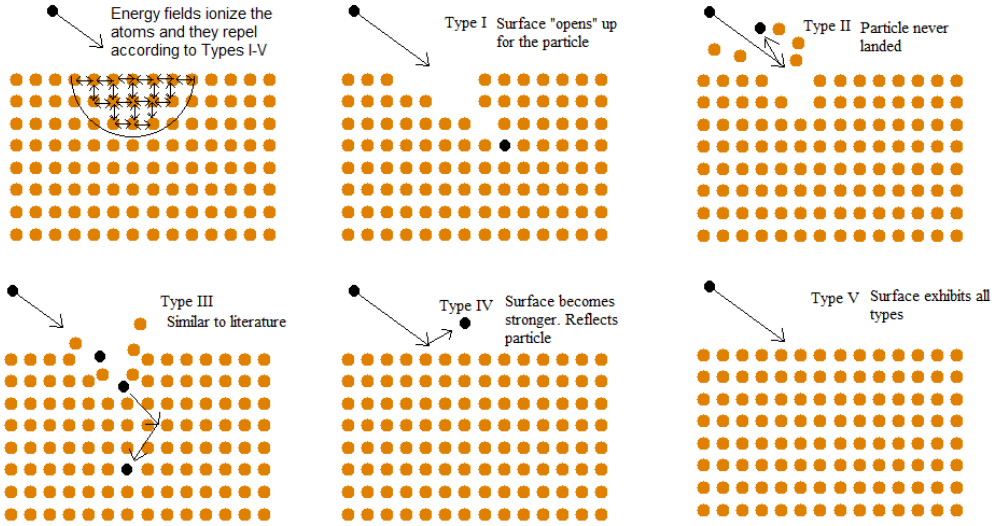

Fig 11: Literature calls it scattering/sputtering, we call it stages of 5 different variants of repulsion starting with ionization of a group of atoms. Literature does not explain the causes of sputtering, we did.

References

[1] Khuram Ali, Sohail A. Khan, M. Z. Mat Jafri; *Effect of Double Layer (SiO2/TiO2) Anti-reflective Coating onSilicon Solar Cells*. Int. J. Electrochem. Sci., 9 (2014) 7865 – 7874

[2] Shuaijun Pan, Arun K. Kota, Joseph M. Mabry, and AnishTuteja*Superomniphobic Surfaces for Effective Chemical Shielding*J. Am. Chem. Soc., 2013, 135 (2), pp 578-581 DOI: 10.1021/ja310517s

[3] Sundberg, Jonas and Cameron, Lisa J. and Southon, Peter D. and Kepert, Cameron J. and McKenzie, Christine J.,*Oxygen chemisorption/desorption in a reversible single-crystal-to-single-crystal transformation*. Chem. Sci., 2014,5, 4017-4025 DOI: 10.1039/C4SC01636J

[4] Kevin A. Arpin, Mark D. Losego, Andrew N. Cloud, HailongNing, Justin Mallek, Nicholas P. Sergeant, Linxiao Zhu, Zongfu Yu, Ber\c c Kalanyan, Gregory N. Parsons, Gregory S. Girolami, John R. Abelson, Shanhui Fan, Paul V. Braun. *Three-dimensional self-assembled photonic crystals with high temperature stability for thermal emission modification.* Nature Communications, 2013; 4 DOI: 10.1038/ncomms3630.

[5] Kim, S., Nam, J. A., Lee, S., In, I. and Park, S. Y. (2014), *Antimicrobial Activity of Water Resistant Surface Coating from Catechol Conjugated Polyquaternary Amine on Versatile Substrates.* J. Appl. Polym. Sci., 131, 40708 doi: 10.1002/app.40708

[6] Bradley, R. M. and Harper, J. M. E. 1988, *Theory of ripple topography induced by ion- bombardment*, J VacSciTechnol A, Vol. 6, pp. 2390-2395.

[7] Yewande, O. E., Kree, R and Hartmann, A. K. 2006, *Morphological regions and oblique-incidence dot formation in a model of surface sputtering*, Phys. Rev. B, Vol. 73, pp. 115434(1)-115434(8).

[8] Yewande, O. E., Kree, R and Hartmann, A. K. 2007, *Numerical analysis of quantum dots on off- normal incidence ion sputtered surfaces*, Phys. Rev. B, Vol. 75, pp. 155325(1)-155325(8).

[9] William H, Miller, *Quantum dynamics of complex systems*; pnas.0408043102 doi:10.1073.

[10] KuniyasuSaitoh and Hisao Hayakawa, *Simulation of depositions of a Lennard-Jones cluster on a crystalline surface*; Progress in Theoretical physics, Vol. 122, No 5, November 2009.

[11] Nguyen Van Hung; *A method for calculation of Morse potential for fcc, bcc and hcc crystals applied to Debye-Waller factor and equation of state*. Communications in Physics, Vol. 14, No 1 (2004) pp 7-14.

[12] Frank M. Mourits and Frans H.A Rummens; *A critical evaluation of Lennard-Jonnes and Stock Mayer potential parameters and some correlation methods*, Can. J. Chem., 55, 3007 (1997).

[13] Rafil-Tabar H. and Mansoori G.A. *Interatomic potential models for nanos-tructures.* ISBN: 1-58883-001-2. Encyclopedia of Nanoscience and Nano-technology., pages 1-17, 2003.

[14] The Virtual Molecular Dynamics Laboratory Group. Virtual moleculardynamics laboratory v.1.1.3.Downloaded 18th June, 2015 at 4:04am; http://polymer.bu.edu/vmd/Software/ index.html, 6 2015.

[15] Raphael OluwoleAkande, Emmanuel OluwoleOyewande; *Photon absorption potential coefficient as a tool for materials engineering*.Int Nano Lett DOI 10.1007/s40089-016-0190-y.